IS-PORTO 2023 PROCEEDINGS

Proceedings of the 8th International Symposium on DEFORMATION CHARACTERISTICS OF GEOMATERIALS Porto, 3rd - 6th September 2023

Contractancy and shear behavior of extremely loose structure soils with particle breakage in saturated and unsaturated conditions

Itsuki Sato[1], *Reiko* Kuwano[2#], and *Masahide* Otsubo[1]

[1] *Institute of Industrial Science, The University of Tokyo, 4-6-1, Komaba, Meguro, Tokyo, Japan*
[#]*Corresponding author: kuwano@iis.u-tokyo.ac.jp*

ABSTRACT

Pumices with high pore voids of volcanic origin are distributed throughout Japan and are the causal layer of slope failures. In many cases of surface failures, it is difficult to assume that the resulting layers are fully saturated. The high water-holding capacity of the pumice suggests that they were deposited in an unsaturated state with a high degree of saturation. In this study, saturated triaxial compression tests and fully undrained unsaturated triaxial compression tests were conducted on artificially produced pumice and natural pumice while measuring the amount of crushing. This is to clarify the relationship between the crushing and mechanical properties of pumice with porous particles, which are often the cause of such disasters, and their behaviour under unsaturated conditions. The results showed that the pumice stones have an ultra-high pore structure. Moreover, pumice with porous particles reached a steady state under both saturated and highly saturated unsaturated conditions, and the amount of crushing increased under highly saturated unsaturated conditions.

Keywords: volcanic pumice; particle crushing; particle breakage; unsaturated; triaxial test.

1. Introduction

Pumices with high void structures of volcanic origin are distributed in numerous parts of Japan and are the causal layer of slope disasters. Typical examples in recent years include an approximately 10-degree gentle-slope flow landslide in the Takanodai area of Minamiaso Village caused by the Kumamoto Earthquake (Chiaro et al. 2022) and hundreds of slope disasters in Atsuma Town caused by the Hokkaido Eastern Iburi Earthquake (Kawamura et al. 2019). It is important to study the mechanical behaviour of crushable porous granular materials responsible for many of these disasters.

Research on slope flow has been conducted for many years. The phenomenon in which a steady state emerges after the unstable deformation of soil, for example, owing to seismic motion, is called flow failure, and the deformation at that time is called flow deformation (Yoshimine and Ishihara 1998; Cubrinovski and Ishihara 2000). Many studies have been conducted on loose sand, including the conditions that cause liquefaction and flow deformation (e.g. Yoshimine and Ishihara 1998; Cubrinovski and Ishihara 2000; Ishihara 1993; Vaid and Chern 1985; Nakata et al. 1998; Alarcon-Guzman et al. 1988; Hyodo et al. 1994). Castro (1969) conducted tests on loose sand and showed that it eventually reaches a “steady state”, which is used to distinguish dilatancy properties on the $e - \log p'$ plane. Note that the steady state of sand is referred to as the critical state in some studies and is often organised as an extension of the critical state model for clay (Sasitharan et al. 1994). Sasitharan et al. (1994) defined the existence of a state boundary surface between the line connecting the peak intensity and the steady state in undrained monotonic tests of loose sand and arranged the properties of loose sand. Ishihara et al. (1975) showed that in triaxial tests of loose sand, a point appears where the effective mean stress reaches a minimum value, where the dilatancy behaviour changes from contractancy to dilatancy and named this point "phase transformation". When the void ratio of the sand is greater than a certain value, the steady state of the phase transformation can be observed, where both the shear stress and effective mean stress are at a minimum as the shear stress decreases; this transient steady state is called a quasi-steady state (Alarcon-Guzman et al. 1988). Yoshimine and Ishihara (1998) conducted undrained shear tests using a hollow cylinder torsional shear apparatus and a triaxial apparatus. They evaluated the risk of flow failure by defining the ratio between the mean effective stress and the maximum excess pore water pressure at the start of the test as Flow The risk of flow failure has been assessed by defining the flow potential as the ratio of the average effective principal stress at the start of the test to the maximum excess pore pressure. Comparing the hollow cylinder torsional shear and triaxial compression tests, the flow potential is evidently greater in the former at similar density and confining pressure.

Particle crushing has also been studied extensively. Hyodo et al. (1998) noted that when crushable soil is sheared, it follows an undrained stress path similar to that of less-crushable loose sand. Particle crushing has a significant impact on the critical state (steady state) because soil gradation is better graded by particle crushing, which allows the soil particles to fill more

efficiently (Bandini and Coop 2011). An index for quantifying the amount of particle crushing is the relative crushing rate Br, as proposed by Hardin (1985). Br has been used in numerous studies because it can easily assess the amount of fracturing simply by sieving. Coop and Lee (1993) and Vilhar et al. (2013) noted that Br in sand is closely related to stress.

In general, soils with porous particles, such as volcanic granular soils, are known to experience particle crushing even at relatively low-pressure levels compared to sand. In porous particles, particle shape changes and changes in the particle array structure are also more pronounced with crushing; therefore, particle crushing significantly affects the shear properties at pressure levels in the normal engineering range (Hyodo et al. 1996). Miura and his research group in Japan proposed a void structure model that divides pumice voids into interparticle and intraparticle void ratios and expresses them as e_{inter} and e_{intra}, respectively (Nakata and Miura 2007; Ishikawa and Miura 2011). Fig. 1 shows its schematic diagram. In cases of surface slope failure of pumice, it is difficult to assume that the resulting layer was fully saturated. Moreover, given the high-water holding capacity of pumice, it was deposited in unsaturated conditions with a high degree of saturation in many cases. Therefore, it is also important to research unsaturated conditions. Grozic et al. (1999) conducted unsaturated fully undrained triaxial tests to determine the shear properties of loosely deposited sands containing gases that cause slope failure at the seabed and showed that high saturation cases lead to a critical steady state (Yoshimine and Ishihara 1998). Matsumaru et al. (2021) and Kazama et al. (2006) conducted repeated shear tests on volcanic soils under fully undrained conditions and showed that even unsaturated soils can liquefy if they are highly saturated.

Research on these porous pumices has not investigated the relationship between the mechanical properties and the amount of particle crushing, partly because of the heterogeneity of the samples collected from natural deposits. In this study, saturated undrained triaxial compression tests and unsaturated fully undrained triaxial compression tests were conducted on natural and artificial pumice. The amount of crushing before and after the tests was measured to investigate the risk of flow failure in naturally deposited porous granular materials at high degrees of saturation.

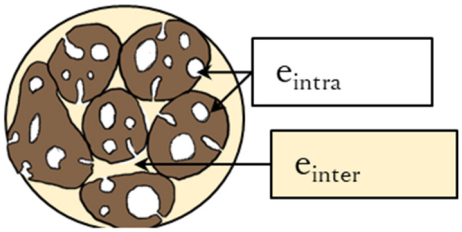

Figure 1. Void structure of porous particles.

2. Materials

2.1. Atsuma pumice (Ta-d pumice)

The Hokkaido Eastern Iburi Earthquake of September 2018 caused numerous ground disasters, particularly in Atsuma, where numerous slope failures with long-range flows occurred over a wide area (Li et al. 2020; Kawamura et al. 2019). In this study, a field survey was conducted on 12 October 2018 at the location of a collapsed slope with a gentle slope of 5°–15° and a flow of approximately 150 m. The Ta-d layer, which is responsible for several landslides (henceforth, "Atsuma pumice"), was sampled (Li et al. 2020; Kawamura et al. 2019; Osanai et al. 2019).

2.2. Artificial pumice

In general, undisturbed samples collected in situ are heterogeneous, with different properties for each sample, even if collected from the same point. Furthermore, the soil and particle structures were disturbed during collection. In this study, to systematically investigate the behaviour of pumice with porous particles, an artificial pumice that could be used to produce a large number of homogeneous samples was prepared. Because many pumice materials that cause disasters have low viscosity or are non-plastic, DL-Clay, an unplastic fine-grained soil, was used as the material for the artificial pumice. DL Clay is one of the clay products marketed by SHOWA KDE CO., LTD. and is used as an experimental material for non-plastic fine-grained soil in many studies in Japan. Artificial soil with crushable soil particles solidified between fine particles was prepared by hand mixing the non-plastic fine-grained soil (DL Clay), rapidly hardened Portland cement, and water in a mass ratio of 85:15:25 for 10 min. It was subsequently sieved with a 2-mm opening and cured in a wet condition for seven days. After seven days of curing, the artificial coarse particles, which were formed by the solidification of the fine-grained soil, were also weakly cemented together. They were vibrated to release the cementation between the coarse particles and subsequently placed in a drying oven for 24 h. The material was then sieved using sieves with openings of 2 mm, 850 μm, and 425 μm.

2.3. Physical properties of materials

Table 1 lists the physical properties of experimental materials. For undisturbed sampling, Pushing Down Type Block Sampling (JGS1231) was used. The paraffin method (JGS 0191) was used to measure e_{intra} (intra-void ratio). The specimens were dipped into a hot paraffin liquid with completely dried porous soil particles to form a film on the surface and prevent water from entering the soil particles.

Table 1. Physical properties

	e_{intra}	G_s	Tested particle size (mass ratio)
Artificial Pumice	-	2.69	2.00 mm–850 μm (70%) 850 μm–425 μm (30%)
Atsuma Pumice (Ta-d)	2.97	2.57	4.75 mm–2 mm (100%)

The water displacement method was then used to determine e_{intra} of the porous particles. The e_{intra} was calculated from the specific gravity, soil particle density, and dry weight of the particles. The e_{intra} of the Atsuma pumice was the average of five pumice particles (average diameter, 6.88 mm).

The intra-void ratio was not measured for the artificial pumice because its small particle size made it difficult to implement the technique using a paraffin solution. Table 2 lists the experiments. Unsaturated tests were conducted under fully undrained conditions, which means that both air and water were undrained.

Table 2. Test list

Specimen	Test type		Sr (%) at compression start	Confining Pressure (kPa)	Test ID
	Consolidation	Compression			
Artificial	Drained	-	100	20, 300, 500	pAC20Br, pAC300Br, pAC500Br
Artificial	Drained	Drained	100	20, 100, 200	pACD20Br, pACD100Br, pACD200Br
Artificial	Drained	Undrained	100	20, 50, 100, 200, 300	pACU20Br, pACU50Br, pACU100Br, pACU200Br, pACU300Br
Artificial	Drained	Fully Undrained	80	20, 100, 200	pA80UCU20Br, pA80UCU100Br, pA80UCU200Br
Artificial	Drained	Fully Undrained	90	20, 100, 200, 300	pA90UCU20Br, pA90UCU100Br, pA90UCU200Br, pA90UCU300Br
Atsuma	Drained	-	100	30, 100, 200, 400	AtsumaC30Br, AtsumaC100Br, AtsumaC100Br, AtsumaC200Br, AtsumaC400Br
Atsuma	Drained	Drained	100	30, 100, 200	AtsumaCD30Br, AtsumaCD100Br, AtsumaCD200Br
Atsuma	Drained	Undrained	100	30, 100, 200	AtsumaCU30Br, AtsumaCU100Br, AtsumaCU200Br
Atsuma	Drained	Fully Undrained	90	20, 100, 200	Atsuma90UCU20Br, Atsuma90UCU100Br, Atsuma90UCU200Br
Atsuma	Drained	Fully Undrained	80	30, 100, 200	Atsuma80UCU30Br, Atsuma80UCU100Br, Atsuma80UCU200Br

2.4. Triaxial compression test apparatus

For the unsaturated triaxial test, a double-cell unsaturated triaxial compression test apparatus developed by the Institute of Industrial Science (IIS) at the University of Tokyo was used (Wang et al. 2016). Regarding the adjustment of saturation degree in the unsaturated test, the soil was saturated as in the CD and CU tests until consolidation, after which the cap side was evacuated before the shear test started. Negative pressure was then applied from the pedestal side to drain water until a predetermined degree of saturation was reached. For the saturated triaxial tests, the double-cell device was removed using the same test apparatus (Wang et al. 2016).

In general, Bishop's effective stress equation was used to calculate the effective stress of unsaturated soils by considering the effects of suction (Fredlund et al. 2012; Bishop et al. 1960). However, it has been pointed out that in pumice stone tests under fully undrained and undrained conditions, the measured values from pore pressure gauges may differ from theoretical values because the air pressure in the void is not constant in the element, and the measured values may not be used as they are (KAZAMA et al. 2006). Therefore, for simplicity, the pore pressure measured from the pedestal side was used as a representative value of the void pressure to calculate the mean effective stress. The moisture characteristic curve in Fig. 2 shows that in the saturation range of this study (80%–100%), the suction during the compression process was sufficiently low relative to the confining pressure below 2 kPa. Note that there was no difference in the conclusions when the air pressure was considered as the void pressure. Fig. 2 shows the water retention curves for different soil gradations in the experiments.

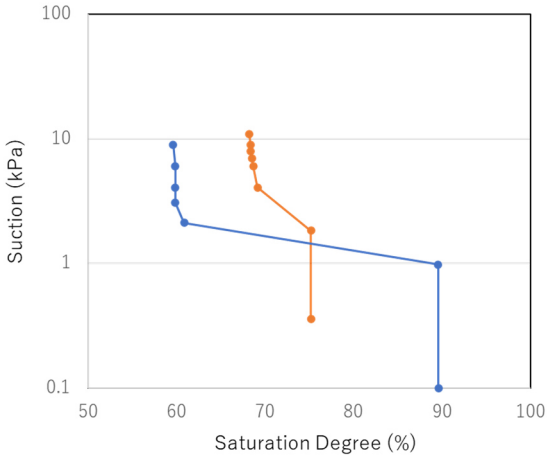

Figure 2. Water retention curves of tested pumice at the soil gradation in the experiments.

2.5. Sample Preparation for Triaxial Tests

For the triaxial tests, artificial pumice specimens with a 50-mm diameter and 100-mm height were prepared by a 20-cm air pluviation method with soil gradation adjusted so that 70% of the grains were 2 mm to 850 μm in diameter, and 30% were 850 μm to 425 μm in diameter

by mass. Air pluviation was used because it is less likely to cause particle crushing than other methods such as tamping.

For Atsuma pumice, only grain sizes between 4.75 mm and 2 mm were used. To avoid particle crushing as much as possible during the specimen preparation process, a metal mould with a 50-mm diameter and 100-mm height was finely rammed with a hammer to vibrate and densify the specimen while particles were gradually added from above with a spoon.

3. Results and Discussions

3.1. Results of Triaxial Tests

The results of the triaxial compression tests on the Atsuma pumice are shown in Fig. 3, and those of the artificial pumice are shown in Fig. 4. The saturated drained tests showed volumetric shrinkage in all cases, except for the low constraining pressure below 30 kPa, and both pumices exhibited high contractancy. For thick pumice with a confining pressure above 100 kPa, the deviator stress (q) continued to increase and did not reach a critical state up to an axial strain of 20 %. In the saturated undrained tests, both pumice stones showed a stress path similar to that of very loose sand; above an axial strain of approximately 10%, they reached a steady state, where the strain progressed with constant deviator stress and mean effective stress. In both pumices, the mean effective stress moved in a decreasing direction after compression started. In the Atsuma pumice, the position on the stress path of the phase transformation coincided with the steady state. This behaviour has a high potential for flow failure.

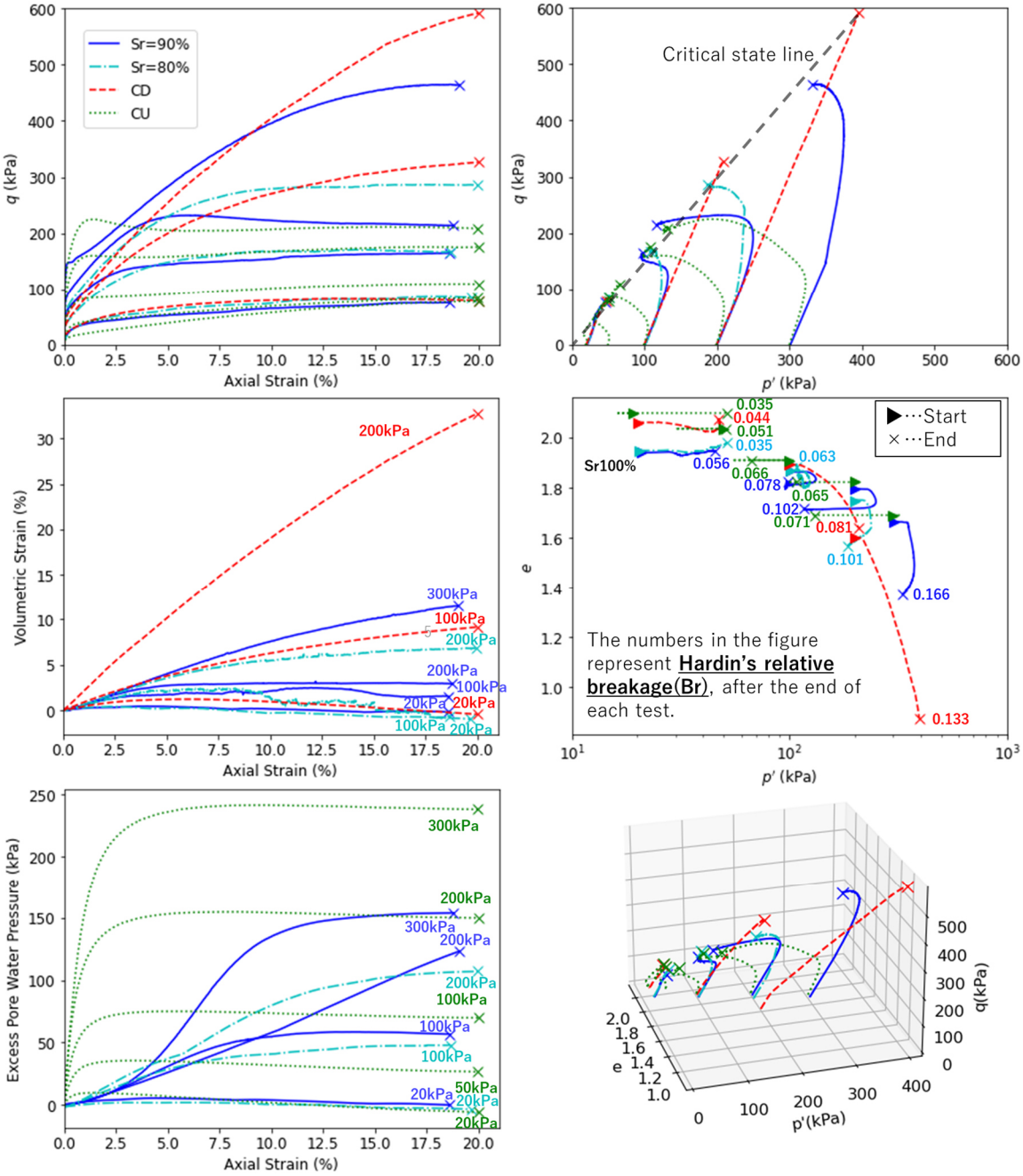

Figure 3. Triaxial compression results of artificial pumice.

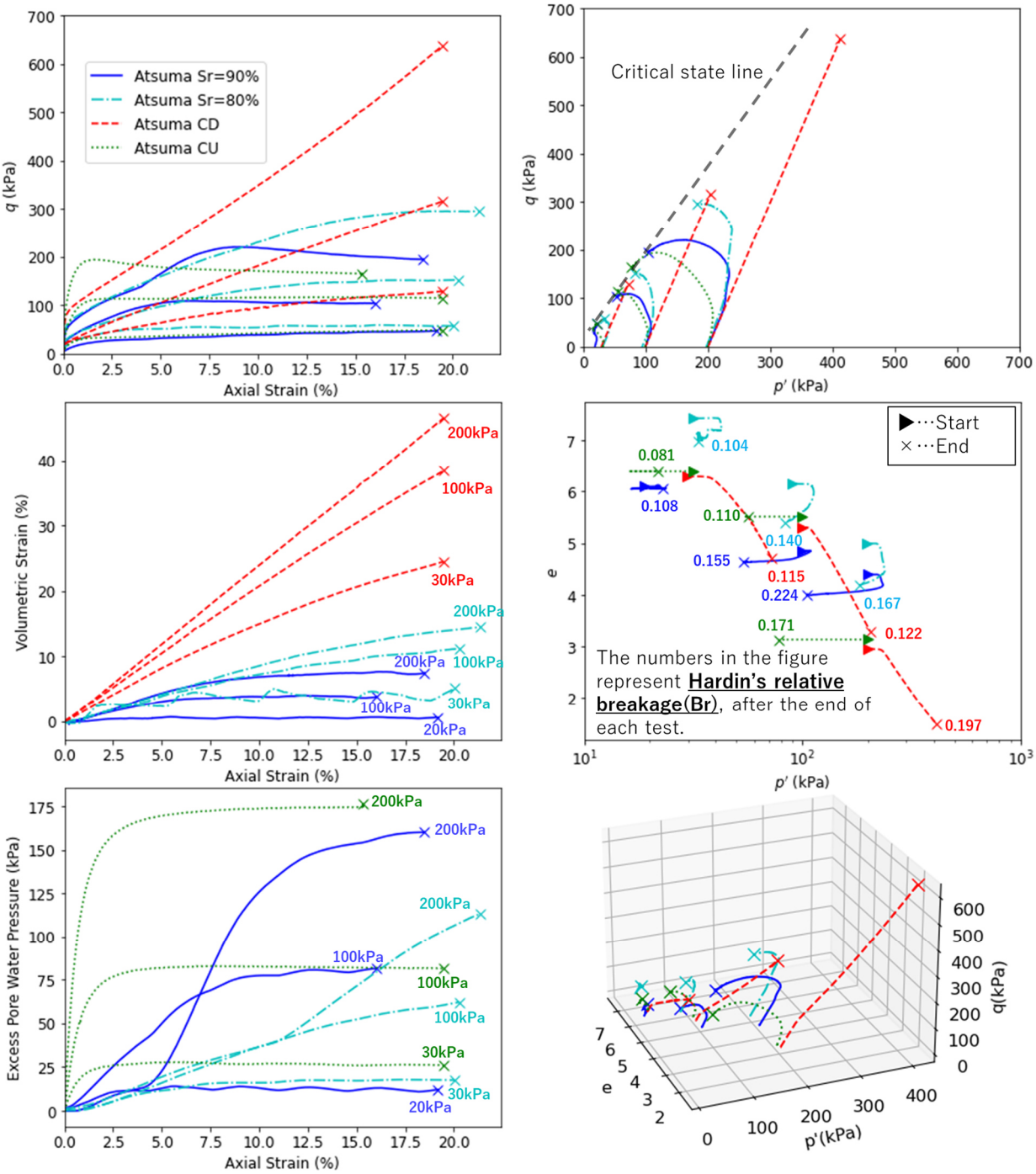

Figure 4. Triaxial compression results of Atsuma pumice.

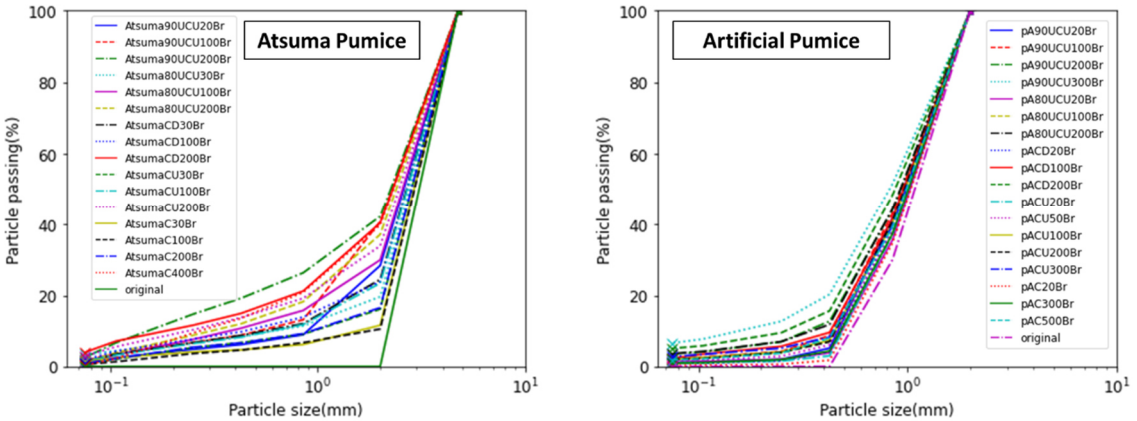

Figure 5. Final particle size distribution curves.

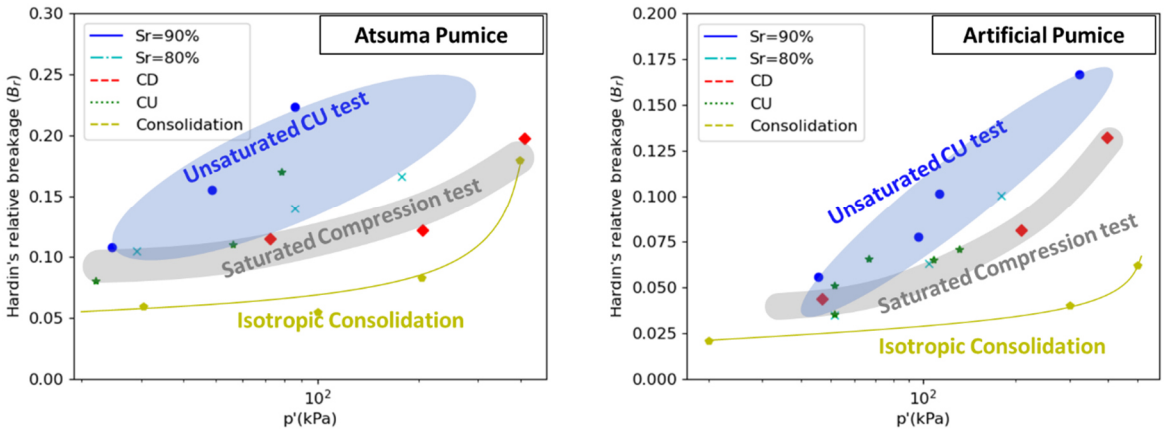

Figure 6. Hardin's relative breakage - p' at the end of tests.

Under unsaturated conditions, the behaviour is almost the same as in undrained tests with loose sand, except for the volumetric strain, leading to a steady state. Regarding the 90% and 80% saturation degree cases, the void ratio decreased from the initial state at confining pressures of 200 kPa and higher, eventually reaching a steady state. The progressive volumetric shrinkage as the void air compresses while following a stress path similar to that of extremely loose sand, which causes flow deformation, is considered to be a particular behaviour observed in unsaturated soils with an extremely loose structure.

Furthermore, in the unsaturation test of the Atsuma pumice at 80% saturation, the stress state (q, p') eventually reached a steady state; however, only the axial strain increased, and the volume shrinkage continued. This state is close to the steady state but differs from the original definition in that the volume continues to shrink. The same stress response as that of the critical steady state (Yoshimine and Ishihara 1998), which is likely to result in flow deformation, was observed in the Atsuma pumice with volume shrinkage.

3.2. Relationship between particle crushing and stress

The $e - \log p'$ curves in Figs. 2 and 3 show that the critical state line is not fixed to one line for either the artificial or Atsuma pumice. This may be because the amount of crushing, soil gradation, and position of the CSL on the $e - log\, p'$ are different in each case.

Fig. 5 shows the post-test particle size distribution in each case. It can be observed that particle crushing has occurred in both artificial and Atsuma pumices. Fig. 6 shows the Hardin's relative particle crushing (Br) in each case plotted at p' at the end of the test. An increase in particle crushing with increasing pressure was observed, which can be represented by the curves in the plots for the isotropic consolidation test and the CD and CU tests, respectively. In the unsaturation test, the degree of particle crushing tended to be slightly higher. The amount of crushing increased in the following order: highly saturated unsaturated compaction ≥ saturated compaction ≥ isotropic compaction. The reason for the increased amount of crushing in the highly saturated unsaturated compression process compared to saturated is unclear; however, one hypothesis is that the volume contraction of the pore air within the particles in response to the increase in pore pressure causes particle crushing.

4. Conclusions

In this study, isotropic consolidation, CD, CU, and unsaturated fully undrained compaction tests were performed on Atsuma and artificial pumices to determine the particle crushing and mechanical behaviour of pumice with porous particles. The following conclusions were drawn:

- Pumice with porous particles is highly compressible and follows the same shape stress path as loose sand without particle crushing in undrained tests, leading to a steady state.
- Pumices with porous particles have high compressibility. Even under unsaturated conditions, air is sufficiently compressible until the pore pressure increases to saturation levels above 80%, which results in an increase in pore air pressure (≈ pore pressure) and contractive behaviour similar to the saturated CU test, leading to a steady state.
- Furthermore, in the unsaturated test of the Atsuma pumice at 80% saturation, the stress state (q, p') eventually reached steady values; however, only the axial strain increased, and the volume shrinkage continued. This state is close to the steady state but differs from the original definition in that the volume continues to shrink.
- Graphically representing Hardin's relative particle crushing and mean effective stress at the end of the test, the isotropic consolidation and saturated compression tests can each be represented by a single curve, with the amount of crushing increasing in the following order: highly saturated unsaturated shear ≥ saturated shear ≥ isotropic consolidation.

The results of this study show that low-pressure, crushable porous soils are extremely compressible that above a certain degree of saturation, they follow the same undrained stress path as loose sand, which causes flow deformation, even under unsaturated conditions. In general, unsaturated soils are considered safer than saturated soils when considering slope failures; however, further investigation is required for crushable porous soils, as they may lead to flow failure even under unsaturated conditions.

References

Alarcon-Guzman, A., Leonards, G.A., and Chameau, J.L. 1988. Undrained Monotonic and Cyclic Strength of Sands. Journal of Geotechnical Engineering, 114(10): 1089–1109.

Bandini, V., and Coop, M.R. 2011. The Influence of Particle Breakage on the Location of the Critical State Line of Sands. Soils and Foundations, 51(4): 591–600. http://doi.org/10.3208/sandf.51.591.

Bishop, A.W., Alpan, I., Blight, G.E., and Donald, I.B. 1960. Factors Controlling the Strength of Partly Saturated Cohesive Soils. In Research Conference on Shear Strength of Cohesive Soils. ASCE. pp. 503–532.

Castro G. 1969. Liquefaction of Sands. Harvard University, Harvard Soil. Mech. Ser. 81, (January 1969).

Chiaro, G., Kiyota, T., Umar, M., and Cappellaro, C. 2022. Earthquake-Induced Flow-Type Slope Failure in Weathered Volcanic Deposits—A Case Study: The 16 April 2016 Takanodai Landslide, Japan. Geosciences, 12(11): 394. http://doi.org/10.3390/geosciences12110394.

Coop, M.R., and Lee, I.K. 1993. The behaviour of granular soils at elevated stresses. In Proceedings of the Wroth Memorial Symposium, Oxford, England, 1992, (1990): pp. 186–198. http://doi.org/10.1680/psm.19164.0012.

Cubrinovski, M., and Ishihara, K. 2000. Flow Potential of Sandy Soils with Different Grain Compositions. Soils and Foundations, 40(4): 103–119. http://doi.org/10.3208/sandf.40.4_103.

Fredlund, D.G., Rahardjo, H., and Fredlund, M.D. 2012. Unsaturated Soil Mechanics in Engineering Practice. In Unsaturated Soil Mechanics in Engineering Practice. John Wiley & Sons, Inc., Hoboken, NJ, USA.

Grozic, J.L., Robertson, P.K., and Morgenstern, N.R. 1999. The behavior of Loose Gassy Sand. Canadian Geotechnical Journal, 36(3): 482–492. http://doi.org/10.1139/cgj-36-3-482.

Hardin, B.O. 1985. Crushing of Soil Particles. Journal of Geotechnical Engineering, 111(10): 1177–1192. http://doi.org/10.1061/(ASCE)0733-9410(1985)111:10(1177).

Hyodo, M., Aramaki, N., Okabayashi, T., Nakata, Y., and Murata, H. 1996. Steady State and Liquefaction Strengths of Crushable Soils. Doboku Gakkai Ronbunshu, 1996(554): 197–209. http://doi.org/10.2208/jscej.1996.554_197.

Hyodo, M., Hyde, A.F.L., and Aramaki, N. 1998. Liquefaction of crushable soils. Géotechnique, 48(4): 527–543. Thomas Telford Ltd.

Hyodo, M., Tanimizu, H., Yasufuku, N., and Murata, H. 1994. Undrained Cyclic and Monotonic Triaxial Behaviour of Saturated Loose Sand. Soils and Foundations, 34(1): 19–32. http://doi.org/10.3208/sandf1972.34.19.

Ishihara, K. 1993. Liquefaction and flow failure during earthquakes. Géotechnique, 43(3): 351–451. http://doi.org/10.1680/geot.1993.43.3.351.

Ishihara, K., Tatsuoka, F., and Yasuda, S. 1975. Undrained Deformation and Liquefaction of Sand Under Cyclic Stresses. Soils and Foundations, 15(1): 29–44. http://doi.org/10.3208/sandf1972.15.29.

Ishikawa, T., and Miura, S. 2011. Influence of Freeze-Thaw Action on Deformation-Strength Characteristics and Particle Crushability of Volcanic Coarse-Grained Soils. Soils and Foundations, 51(5): 785–799. http://doi.org/10.3208/sandf.51.785.

Kawamura, S., Kawajiri, S., Hirose, W., and Watanabe, T. 2019. Slope Failures/Landslides Over a Wide Area in the 2018 Hokkaido Eastern Iburi Earthquake. Soils and Foundations, 59(6): 2376–2395. Japanese Geotechnical Society. http://doi.org/10.1016/j.sandf.2019.08.009.

Kazama, M., Takamura, H., Unno, T., Sento, N., and Uzuoka, R. 2006. Liquefaction Mechanism of Unsaturated Volcanic Sandy Soils. Doboku Gakkai Ronbunshuu C, 62(2): 546–561. http://doi.org/10.2208/jscejc.62.546.

Li, R., Wang, F., and Zhang, S. 2020. Controlling Role of Ta-d Pumice on the Coseismic Landslides Triggered by 2018 Hokkaido Eastern Iburi Earthquake. Landslides, 17(5): 1233–1250. Landslides. http://doi.org/10.1007/s10346-020-01349-y.

Matsumaru, T., Unno, T., and Midorikawa, Y. 2021. Numerical Simulation of Unsaturated Liquefaction Test Using Volcanic Soils Damaged in the 2018 Hokkaido Iburi Eastern Earthquake. Journal of Japan Society of Civil Engineers, Ser. A1 (Structural Engineering & Earthquake Engineering (SE/EE)), 77(4): I_533-I_543. http://doi.org/10.2208/jscejseee.77.4_I_533.

Nakata, T., and Miura, S. 2007. Change in Void Structure Due to Particle Breakage of Volcanic Coarse-Grained Soil and Its Evaluation. Doboku Gakkai Ronbunshuu C, 63(1): 224–236. http://doi.org/10.2208/jscejc.63.224.

Nakata, Y., Hyodo, M., Murata, H., and Yasufuku, N. 1998. Flow Deformation of Sands Subjected to Principal Stress Rotation. Soils and Foundations, 38(2): 115–128. http://doi.org/10.3208/sandf.38.2_115.

Osanai, N., Yamada, T., Hayashi, S. ichiro, Kastura, S., Furuichi, T., Yanai, S., Murakami, Y., Miyazaki, T., Tanioka, Y., Takiguchi, S., and Miyazaki, M. 2019. Characteristics of Landslides Caused by the 2018 Hokkaido Eastern Iburi Earthquake. Landslides, 16(8): 1517–1528. Landslides. http://doi.org/10.1007/s10346-019-01206-7.

Sasitharan, S., Robertson, P.K., Sego, D.C., and Morgenstern, N.R. 1994. State-Boundary Surface for Very Loose Sand and Its Practical Implications. Canadian Geotechnical Journal, 31(3): 321–334. http://doi.org/10.1139/t94-040.

Vaid, Y.P., and Chern, J.C. 1985. Cyclic and Monotonic Undrained Response of Saturated Sands. In Advances in the Art of Testing Soils Under Cyclic Conditions. pp. 120–147.

Vilhar, G., Jovičić, V., and Coop, M.R. 2013. The Role ofParticle Breakage in the Mechanics of a Non-Plastic Silty Sand. Soils and Foundations, 53(1): 91–104. http://doi.org/10.1016/j.sandf.2012.12.006.

Wang, H., Sato, T., Koseki, J., Chiaro, G., and Tan Tian, J. 2016. A System to Measure Volume Change of Unsaturated Soils in Undrained Cyclic Triaxial Tests. Geotechnical Testing Journal, 39(4): 20150125. http://doi.org/10.1520/GTJ20150125.

Yoshimine, M., and Ishihara, K. 1998. Flow Potential of Sand During Liquefaction. Soils and Foundations, 38(3): 189–198. http://doi.org/10.3208/sandf.38.3_189.